Search for photon primaries with The Pierre Auger Observatory

P. Bernardini [1 2] C. Bleve[12 3] G. Cataldi[2], M. R. Coluccia[12], A. Corvaglia, [2] P. Creti,[2] S. D'amico[4 2], I. De Mitri[12], U. Giaccari[12], G. Mancarella[12], G. Marsella [42], D. Martello[12], M.Panareo[42], L.Perrone[42], C. Pinto[42], M. Settimo[12 5] and the AUGER Collaboration

[1]Dipartimento di Fisica, Università del Salento, Italy

[2]Istituto Nazionale di Fisica Nucleare sez. di Lecce, Italy,

[3]now at the Dept. of Physics, Bergische Universität Wuppertal, Germany ,

[4]Dipartimento di Ingegneria dell'Innovazione, Università del Salento, Italy

[5]now at the Dept. of Physics, University of Siegen, Germany ,

1. Introduction

All the scenarios invoked to explain the origin of Ultra-High Energy Cosmic Rays (UHECR) predict fractions of primary photons, along with a nuclear component. The expected fluxes depend primarily on the chemical composition of primaries and on the nature, cosmological evolution and spatial distribution of astrophysical sources [1–4].

A guaranteed flux of photons is expected from the interaction of UHECRs with the cosmic microwave background, the GZK effect [5]. In particular, cosmic rays above $\sim 5 \cdot 10^{19}$ eV may exceed the threshold for resonant $\Delta+$ particle production. These unstable secondaries decay into pions and subsequently into photons and neutrinos. Both photons and neutrinos point back to the sites of production, revealing details of the sources and of their acceleration mechanisms. Photon detection at the Earth would also deliver information on extragalactic radio background and magnetic fields. By probing aspects of high-energy interactions it would have large impact also on fundamental physics [6].

Identification of photons is possible, by observing deviations of the recorded data from expectations relative to showers induced by nuclear primaries. By combining the fluorescence and the surface array detection techniques in a hybrid instrument, the Pierre Auger Observatory has a unique potential for this kind of searches. The southern site of the Observatory, consisting of a surface detector with 1600 water-Cherenkov stations extending over 3000 km^2 on a triangular grid (1.5 km spacing), and of a fluorescence detector overlooking the array with 24 fluorescence telescopes hosted in four sites, is stably taking data since January 2004.

So far no observation has been claimed, but stringent limits on fraction and absolute flux of primary photons have been placed [7–9]. These limits put severe constraints to non-acceleration models [10] and favor astrophysical scenarios for the origin of the highest particles.

The group of Lecce was involved in this analysis, in particular in search for photon primaries with the fluorescence detector operating in hybrid mode. The main activities of the group concerning this topic are outlined and summarized below.

2. Search for photons with the Fluorescence Detector

Distinctive characteristics of photon induced showers are a deeper shower maximum, $X_{\max}$, and a poorer muonic component. The delayed development of photon showers with respect to hadronic is due to the smaller multiplicity in electromagnetic interactions, and it is further delayed by the LPM effect [11] above 10 EeV. A dominating electromagnetic component is expected due to the lower cross sections both for photo-nuclear interactions and muon pair production.

2.1. Upper limits on photon fraction

The key observable in searches for photon primaries with the Auger fluorescence detector is $X_{\max}$ itself [7]. Since the fluorescence telescopes follow the longitudinal shower development, the derivation of the depth of maximum can be performed with very high accuracy [12]. The procedure highly benefits from the small uncertainty in the geometry reconstruction of hybrid events, i.e. those events recorded by both the fluorescence telescopes and the surface array.

In Fig. 1 the distribution of $X_{\max}$, is plotted for samples of Monte Carlo showers induced by photons (solid blue line), protons (dashed red line) and iron nuclei (dotted black line) at 10 EeV. The difference between the average $X_{\max}$ value for showers induced by protons and photons at this energy is ~ 200 g cm^{-2}, which is large compared to the $X_{\max}$ resolution of the hybrid detec-

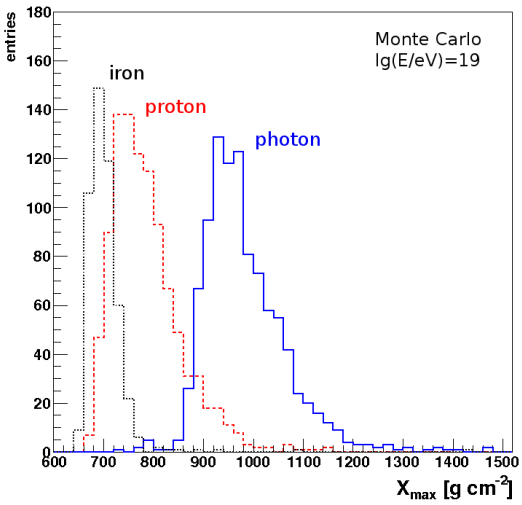

Figure 1. Discriminating observable for photons in the Auger fluorescence detector: the depth of shower maximum, $X_{\rm max}$. Distribution of $X_{\rm max}$ are shown for Monte Carlo events induced by photons (solid blue line), protons (dashed red line) and iron nuclei (dotted black line) at 10 EeV.

tor, ~ 20 g cm^{-2} [13].

Observations in hybrid mode are possible also at energies below 10 EeV. By decreasing the energy threshold, the event statistics increases balancing, to some extent, the factor $\sim$10 smaller duty cycle compared to observations with the ground array alone. A high quality hybrid data sample was selected applying a set of cuts on reconstruction quality, fiducial volume and cloud coverage (for details see Ref. [9]). The observed $X_{\rm max}$ of all the photon-like events was compared to expectations from photon induced showers with the same geometry and energy. 8, 1, 0, 0 photon candidate events were found with energies greater than 2, 3, 5 and 10 EeV, respectively. Their number was found to be compatible with expectations from nuclear background.

Upper limits of 3.8%, 2.4%, 3.5% and 11.7% on the fraction of cosmic-ray photons above 2, 3, 5 and 10 EeV were obtained at 95% c.l., see Ref. [9]. The hybrid limits (Auger HYB) are shown in Fig. 2 together with the surface array limits (Auger SD), other experimental results, model predictions and GZK bounds.

We studied the robustness of the results against different sources of uncertainty. Varying individual event parameters or the selection criteria, within the experimental resolution, leaves the results essentially unchanged. The effective total systematic uncertainty in $X_{\rm max}$ for this analysis amounts to $\sim$16 g cm^{-2} (see Ref. [9] for details). By increasing (reducing) all the reconstructed $X_{\rm max}$ values by this value, the number of photon candidates was increased (reduced) only for the two lowest energy samples. Accordingly, the limits become 4.8% (3.8%) above 2 EeV and 3.1% (1.5%) above 3 EeV, while the limits above 5 and 10 EeV are unchanged.

2.2. Upper limits on photon flux

Deriving an upper limit to the photon flux requires a solid knowledge of the detector exposure. For the hybrid detector, it is influenced by several factors, including the atmospheric conditions and all the actual DAQ configurations. The method developed for the measurement of the energy spectrum[14] is applied in this analysis and an accurate evaluation of the hybrid exposure for photon primaries is performed [15]. In fig. 3 the hybrid exposure is shown after quality cuts on reconstructed geometry and longitudinal profile and requiring that the median of reconstructed X_{max} is larger than the expected value from simulations for photon showers. The trigger efficiency for iron is reduced at lower energies due to higher altitude of the average X_{max}. Photons with energies lower than 10^{18} eV tends to be more efficient than hadrons. In this energy range, in fact, they have a higher chance of triggering FD as their $X_{\rm max}$ is generally deeper. For the SD counterpart, the muon content is less and the size of

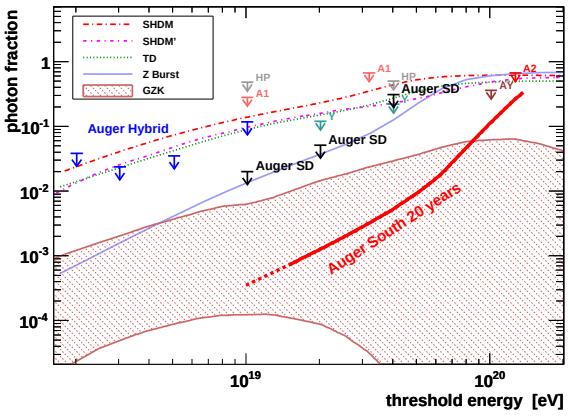

Figure 2. Upper limits on photon fraction in the integral cosmic-ray flux. In black, limits from the Auger surface detector (Auger SD) [8]; in blue, hybrid limits (Auger HYB) [9]. Previous limits from other experiments AGASA (A1, A2), AGASA-Yakutsk (AY), Yakutsk (Y), Haverah Park (HP). Lines indicate predictions from top-down models. The shaded region shows the expected GZK bounds [1]. The solid red line (Auger South 20 years) is an estimate of the sensitivity to UHE photons of the southern Auger site after 20 years of operation, see Ref. [6].

the effective footprint at ground is smaller (about 500 m less at 10^{19} eV), giving a lower chance of triggering at least one stations.

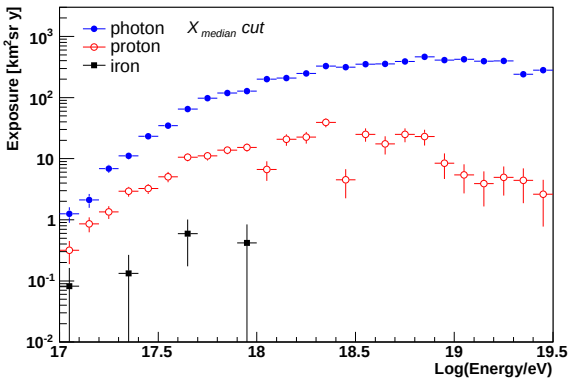

Figure 3. Exposure of the hybrid detector for photon (blue dots) compared to proton (red empty dots) and iron (black squares) after the discrimination of events based on the reconstructed X_{max} [15]

The upper limit is given here in terms of integrated photon flux according to the statistical method developed by Feldman-Cousins [16]. The photon flux integrated above the energy threshold E_0 is given by:

$$\oplus_\gamma(E_\gamma > E_0) = \int_{E_0}^{\infty} \phi_\gamma(E)dE \qquad (1)$$

where ϕ_γ is the differential flux. Taking into account the detector exposure, the observed number of photons with $E_\gamma > E_0$ is:

$$N_\gamma^{obs}(E_\gamma > E_0) = \int_{E_0}^{\infty} \phi_\gamma(E_\gamma) \cdot \mathcal{E}_\gamma(E_\gamma)dE \qquad (2)$$

In a conservative approach, the upper limits on the photon flux can be written as:

$$\oplus_\gamma^{95CL} < \frac{N_\gamma^{95CL}(E_\gamma > E_0)}{\mathcal{E}_{\gamma,min}(E_\gamma > E_0) \cdot \epsilon_{cloud}}. \qquad (3)$$

where $\mathcal{E}_{\gamma,min}$ is the minimum value of the exposure over the integration energy domain. Since the exposure increases monotonically with energy, $\mathcal{E}_{\gamma,min}$ coincides with $\mathcal{E}_\gamma(E_0)$. Table 1 summarizes the number of photon candidates, their upper limits without background subtraction and the minimum value of the photon exposure in each energy interval. The confidence intervals are also computed taking into account the estimated background. For this study the Rolke and Lopez [17,18] statistical method is used. Unlikely the Feldman and Cousins approach, this method deals with a better treatment of the background with its uncertainty.For this study, a Poissonian distribution of the expected background is considered assuming a 50% proton - 50% iron mixed composition for QGSJet-II and QGSJet-I hadronic interaction models. Upper limits of about 10^{-1}, 3.7×10^{-1}, 2.6×10^{-2}, 1.4×10^{-2}, 2.5×10^{-2} km^{-2} sr^{-1} y^{-1} are derived in the conservative approach (red arrows in fig. 4) for energy above 2, 3, 5, 10 and 20 EeV. A weak dependence on the hadronic interaction model is observed. If QGSJet-I is used as hadronic interaction model, these upper limits are about 6.510^{-2}, 3.8×10^{-1}, 2.6×10^{-2}, 1.6×10^{-2}, 2.1×10^{-2} km^{-2} sr^{-1} y^{-1}. Using the flux of cosmic rays measured by Auger [19], these results can be converted into limits on photon fraction. In the corresponding energy bands it gives 1.7%, 2%, 3.5%, 8%, 65%, well in agreement or slightly lower than findings of [9] as this analysis can count on a detailed exposure calculation.

In the hypothesis that the background is subtracted, the upper limits (blue arrows in fig. 4) improve down to 4.7×10^{-2}, 2.2×10^{-2}, 2.2×10^{-2}, 1.12×10^{-2}, 2.1×10^{-2} km^{-2} sr^{-1} y^{-1} using QGSJet-II and down to 2.1×10^{-2}, 3×10^{-2}, 2×10^{-2}, 1.4×10^{-2}, 1.8×10^{-2} km^{-2} sr^{-1} y^{-1} for QGSJet-I above 2, 3, 5, 10 and 20 EeV. The expectations from several theoretical models (dashed and solid lines) are also shown as derived from [20] by integrating the prediction of the differential flux up to 10^{21} eV. Models of Super Heavy Dark Matter (SHDM), Z-Burst (ZB) and Topological Defect (TD) are excluded by these upper limits. They confirm the results of the SD detector (black arrows) at the highest energies where SD has a better sensitivity due to its larger acceptance (i.e. larger duty cycle). Nonetheless, the principal benefit of the hybrid detector is the capability of exploring an energy region currently not accessible to SD. Moreover,

E_0	N_γ	N_γ^{95}	$\mathcal{E}_{\gamma,min}$ [km^{-2} sr^{-1}s]
2 EeV	9	16.78	322.62
3 EeV	2	6.73	352.44
5 EeV	1	5.15	390.85
10 EeV	0	3.09	422.86
20 EeV	0	3.09	241.20

Table 1
Summary of the number of the observed photon candidates N_γ and of the upper limits at 95% C.L. (N_γ^{95CL}) for energy above a given threshold E_0. The minimum value of the exposure $\mathcal{E}_{min}$ in the corresponding energy range is also reported.

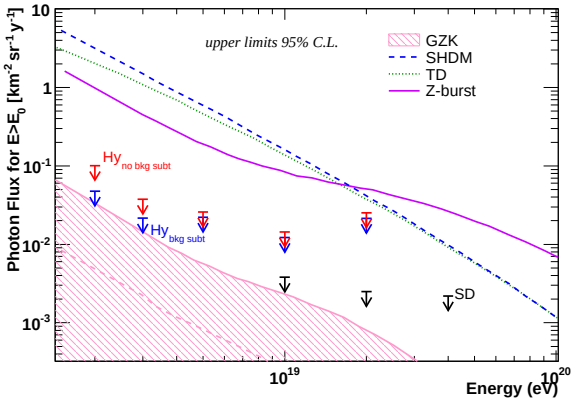

Figure 4. Upper limits at 95% C.L. on the integral photon flux from this analysis (Hyb). Results are shown for both the cases with (blue arrows) and without (red arrows) the hadron background subtraction. Results from SD [8] at the highest energies are also given for comparison. Lines give predictions from top-down models [21] and the shaded region shows the expected GZK bounds [20].

in the case of background subtraction, the upper limits around few EeV are close to the edge of the region of expected photon flux from GZK (dashed area). The given predictions (solid and dashed pink lines [20]) result from a fit to HiRes data for two different hypotheses on the extragalactic proton component and assuming an extragalactic radio background of $B_{EGMF} \sim 10^{-9}$ G.

REFERENCES

1. G. Gelmini, O. Kalashev, and D. V. Semikoz, `arXiv:0706.2181 [astro-ph]`.
2. V.S. Berezinsky *et al.*, Phys. Lett. B 28 (1969) 423.
3. M. Ahlers *et al.*, Astropart. Phys. 34 (2010) 106.
4. K. Kotera, D. Allard, A. V. Olinto `arXiv:1009.1382 [astro-ph.HE]`
5. Greisen, K., Phys Rev Letters, 16 (1966) 748.
6. M. Risse and P. Homola, Mod. Phys. Lett. A 22 (2007), 749.
7. Pierre Auger Collaboration [J. Abraham *et al.*], Astropart. Phys. 27 (2007) 155.
8. Pierre Auger Collaboration [J. Abraham *et al.*], Astropart. Phys. 29 (2008) 243.
9. Pierre Auger Collaboration [J. Abraham *et al.*], Astropart. Phys. 31 (2009) 399.
10. P. Bhattacharjee and G. Sigl, Phys. Rep. 327 (2000), 109.
11. L.D. Landau, I.Ya. Pomeranchuk, Dokl. Akad. Nauk SSSR 92, 535 (1953); Dokl. Akad. Nauk SSSR 92, 735 (1953). A.B. Migdal, Phys. Rev. 103, 1811 (1956).
12. Pierre Auger Collaboration [J. Abraham *et al.*], Phys. Rev. Lett. 104 (2010) 091101.
13. J. Bellido [Pierre Auger Collaboration], 31^{st} ICRC, Łódź, Poland (2009), #124.
14. J. Abraham *et al.* (The Pierre Auger Collaboration), Astroparticle Physics 34 (2011) 368-381
15. PhD. Thesis of Mariangela Settimo, *Hybrid detection of Ultra High Energy Cosmic Rays with the Pierre Auger Observatory*, Physics Department, Università del Salento (Lecce, Italy)
16. G.J. Feldman and R.D. Cousins, Phys.Rev.D. 57, (1998) 3873.
17. W. A. Rolke, A.M. Lopez, J Conrad, Nucl.Instrum.Meth. A551 (2005) 493.
18. J. Lundeberg, J. Conrad, W. A. Rolke, A.M. Lopez, Comp. Phys. Comm. 181 (2010) 683.
19. J. Abraham *et al.* (The Pierre Auger Collaboration), Physics Letters B 685 (2010) 239-246
20. G. Gelmini, O. Kalashev,D. Semikoz, Astropart.Phys.28 (2007), 390.
21. G.Sigl, International School of Cosmic-Ray Astrophysics, Erice (1996), astro-ph/9611190v1